Laser fluence-dependent LIPSS formed on the surface of niobium alloys

Murodbek E. Vapaev[1*], *Furkat M.* Tojinazarov[2], *Bekhzod R.* Sobirov[3], *Shavkat R.* Kamalov[3], *Ikram Y.* Davletov[1], and *Ganjaboy S.* Boltaev[3,4,5]

[1]Department of Technique, Urgench State University, Urgench, Uzbekistan
[2]Center for Advanced Technologies, Tashkent, Uzbekistan
[3]Institute of Ion-Plasma and Laser Technologies, Tashkent, Uzbekistan
[4]Tashkent Institute of Irrigation and Agricultural Mechanization Engineers, National Research University, Tashkent, Uzbekistan
[5]Department of Physics, American University of Sharjah, Sharjah, United Arab Emirates

Abstract. Laser fluence-dependent laser-induced periodic surface structures (LIPSS) on niobium alloys was analysed. Additionally, we explored the shift from LIPSS to self-organized, periodic microstructures resembling cones. The findings shed light on how surface structures in niobium evolve depending on laser fluence. Significantly influence of laser fluence to the gradual transition of low-spatial frequency LIPSS to high-frequency spatial LIPSS was demonstrated. Highly organized LIPSS on the surface of targets was obtained at the higher accumulated fluence of laser pulses.

1 Introduction

The development of periodic nanostructures (LIPSS) on metal surfaces due to laser exposure is a subject of current scientific and research focus. LIPSS refer to self-organized nanostructures that form when laser radiation, close to the ablation threshold for a single pulse, interacts with a material surface. Metal alloys play a significant role in LIPSS research due to their potential impact on the biological response, chemical composition, and consistency of surface patterns produced by femtosecond laser pulses [1,2].

LIPSS are a universal phenomenon that can be observed on almost any material, but metal alloys may have different properties and behaviours than other materials [3,4]. Nanostructures possess numerous functional chemical and physical characteristics that can be harnessed for intricate nanodevices in nanotechnology. These properties vary substantially from those of bulk materials owing to atomic-scale phenomena, such as energy quantization, surface, interference, and single-electron effects [5-8].

This study focuses on niobium, a technologically important metal [9]. Niobium is a light gray, ductile transition metal that can enhance the strength and stability of structural steel when added as a microalloying element [10]. Niobium is a metal known for its ability to improve the properties of niobium alloys, particularly when exposed to low temperatures

* Corresponding author: murodbek.v@urdu.uz

[11]. These alloys find applications in jet engines and rockets, architectural constructions, superconducting wires for pipelines, and superconducting magnets [12]. Niobium is also employed in superconducting radio frequency cavities and various other advanced technologies. To enhance the performance of these devices, modifications to the niobium surface are necessary.

One potential method involves utilizing a laser to induce nanostructure formation on the material surface. The initial texturing of the niobium surface with LIPSS through femtosecond laser multi-pulse ablation slightly above the ablation thresholds has been documented [13]. Femtosecond laser treatment has the capability to modify the surface superconducting characteristics of niobium and may serve as an alternative to traditional methods like electropolishing or buffered chemical polishing [14]. More theoretical and experimental work is needed to develop a precise physical model for Nb surface texturing.

This paper describes an experiment that used a picosecond pulse laser to create periodic nanostructures on the surface of niobium and its alloys under normal conditions.

2 Experimental arrangements

The LIPSS technique was employed to induce the formation of Laser-Induced Periodic Surface Structures on metal alloy surfaces. Solid niobium targets (comprising NbC and NbTaW) were irradiated under normal atmospheric conditions using a Nd:YAG laser (EKSPLA PL-2231-50) with a wavelength of 1064 nm and a pulse duration of 28 ps. The pulse energy ranged from E=0.4 to 4 mJ, resulting in laser fluence values between 2.83 and 28.3 mJ/cm².

The fluence of the laser pulse was determined for a focusing geometry with a focusing lens (F=250 mm) and a beam diameter of d=60 μm on the surface of the bulk targets. A scanning electron microscopy (SEM, TESCAN VEGA3) was utilized to analyze surface morphology after laser ablation process. The spatial frequency of the LIPSS was determined by performing a two-dimensional Fast Fourier Transform (2D-FFT, Gwyddion) of the SEM images perpendicular to the LIPSS direction (Figure 1).

Our samples consisted of NbC and NbTaW metal alloys. Niobium carbide (NbC) is a highly resilient refractory ceramic material utilized in cutting tools and as a grain growth inhibitor in cemented carbides. NbTaW is a ternary alloy composed of niobium, tantalum, and tungsten, characterized by its high melting point, corrosion resistance, and mechanical strength [15].

3 Results and discussion

Figure 1 reveals the SEM elemental analysis EDS spectrum of the NbC and NbTaW alloy surfaces in the solid aggregate state. The percentage of the components in the niobium alloys can be seen in these figures. For NbC, the sample consists of 73% Nb and 20% C. For NbTaW, the alloy components are 11% Ta, 8.2% Nb and 3% W, respectively.

The ablation process on these samples was carried out under normal conditions using a tightly focused 28 ps laser beam. Formed on the surface LIPSS can be divided into two types according to their periodicity sizes: LSFL, where the period of LIPSS equals the wavelength of the ablating laser ($\Lambda \approx \lambda$), and HSFL ($\Lambda << \lambda$), where the period of LIPSS is smaller than the wavelength of the ablating laser [6]. Here, Λ is the LIPSS period and λ is the laser wavelength.

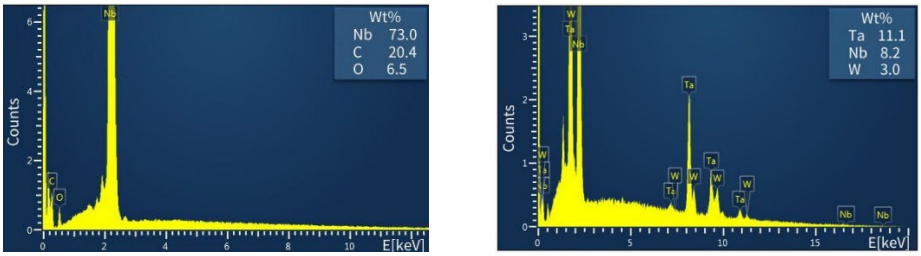

Fig. 1. SEM elemental analysis image of the surface of NbC and NbTaW alloys.

Figure 2 illustrates the SEM image and 2D-FFT analysis of the LIPSS formed on the surface of the NbC alloy while scanning laser beam at the speed of 20 mm/min. The periodicity of Λ =900±100 nm of LSFL was reached on the NbC surface through laser irradiation with an energy density of 2.83 mJ/cm² (Figure 2a). The period of LIPSS did not varied with changes in energy density while maintaining a constant scanning speed on the surface of NbC. At energy densities of 14 and 28 mJ/cm², LSFL with a period of Λ =900±100 nm were observed (Figure 2b,c). It is due to the correlation of electron density in the laser-induced plasma with wavelength of surface plasmon waves. In the case of NbC plasma concentration changes was not enough to inpact periodicity of LIPSS.

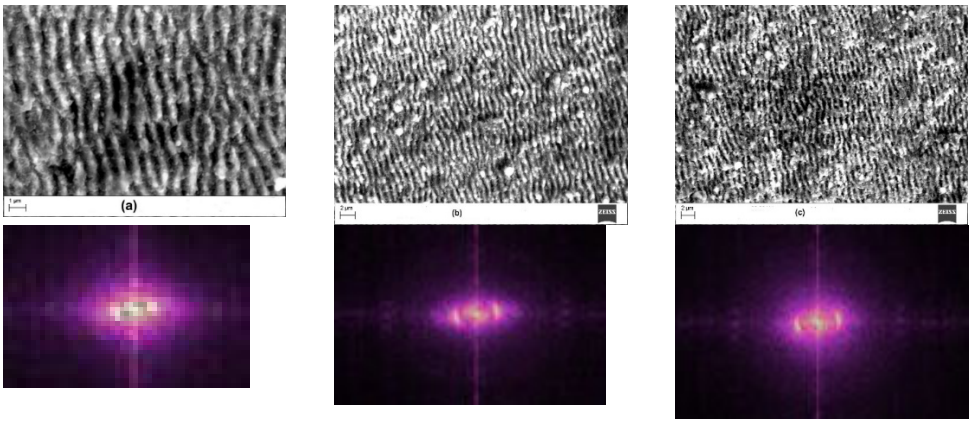

Fig. 2. SEM image and 2D-FFT analysis of NbC alloy surface a) E=0,4 mJ, Λ=600 nm LIPSS (HSFL) b) E=2 mJ, Λ=950 nm LIPSS (LSFL) c) E=4 mJ, Λ=970 nm LIPSS (LSFL).

Figure 3 depicts the SEM image and 2D-FFT analysis of the LIPSS formed on the surface of the NbTaW alloy while scanning at a speed of 20 mm/min. HSFL with an average period of Λ =650±50 nm (Figure 3a) and Λ =750 nm (Figure 3b,c) were achieved on the NbTaW surface through laser irradiation with energy densities of 2.83 and 14-28 mJ/cm², respectively. It is observed that Nb alloy containing tungsten and tantalum shows lower LIPSS periodicity compared to Nb alloy containing carbon atoms.

It can be concluded that alloys with heavy metals can generate plasma containing highly concentrated free electrons, which regulates the dispersion parameters on the target surface. Below we analyze these relationships between electron density, laser-induced plasma dispersion parameters, and LIPSS periodicity.

The 2D-FFT analysis revealed that a periodic truncated cone structure was created on the NbTaW alloy surface (Figure 4). A periodic structure with a height of 250 nm and a base diameter of 650 nm was obtained by 0.4 mJ 28 ps laser pulses.

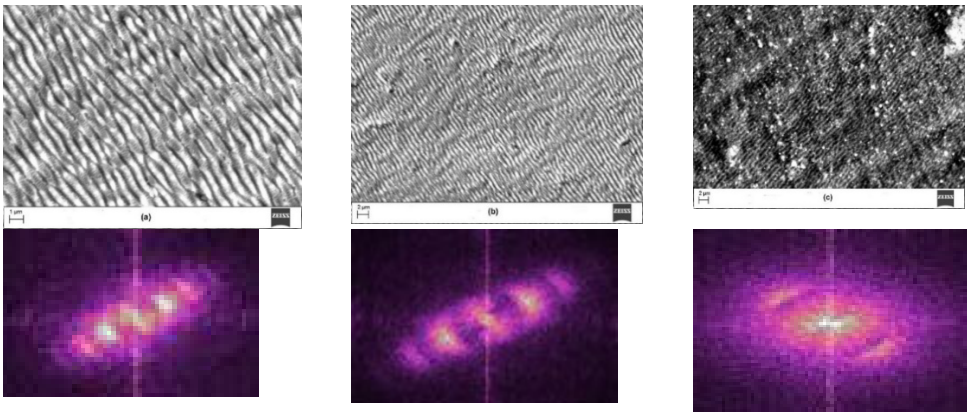

Fig. 3. SEM image and 2D-FFT analysis of NbTaW alloy surface a) E=0,4 mJ, Λ=650 nm LIPSS (HSFL) b) E=2 mJ, Λ=750 nm LIPSS (HSFL) c) E=4 mJ, Λ=750 nm LIPSS (HSFL).

To study a correlation between fluence and LIPSS periodicity might be clerified by analysis laser induced plasma parameters and thier dependence on parameters of surface plasmon polaritions (SPPs). The plasmonic wave's frequency of SPP related to the plasmon frequency(ω_p), the electron density (n_e), the electron's charge (e), the dielictric constant (ε_0), and the mass of the electron (m_e) can be present as following [16]

$$\omega_p(n_e) = \sqrt{\frac{n_e e^2}{\varepsilon_0 m_e}} \tag{1}$$

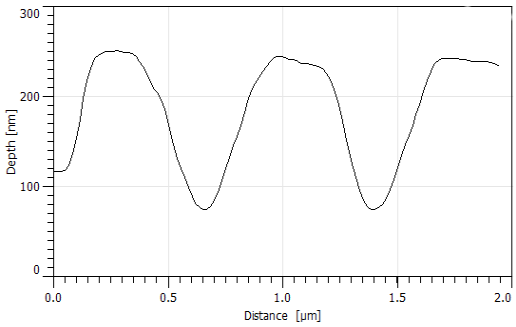

Fig. 4. NbTaW alloy surface is a periodic truncated conical structure.

The surface plasmon frequency is determined by the electron density, which serves as the charge carrier for materials exhibiting specific conductivity. Increased electron density within the plasma fosters the creation of HSFL. Our findings showcase the control over LIPSS formation, opening avenues for novel applications and functionalities of materials structured by pulsed lasers. Therefore, by tuning the plasmonic frequency, the SPP wavelength via tuning the laser-induced plsma paramaters and the LIPSS periodicity can be controlled

$$\Lambda_{LSFL} = \frac{\lambda \cdot \lambda_{SPP}}{\lambda + \lambda_{SPP} \sin(\theta)}; \tag{2}$$

Λ_{LSFL}- LSFL periodicity, λ-laser wavelength,λ_{SPP} SPP wavelength, θ angle of incidence of laser radiation, R- material reflection coefficient, [17,18].

As per this plasmonic model, the plasmon wavelength at the interface of metal and dielectric for a laser incident perpendicular to the surface is determined as

$$\lambda_{SPP} = \lambda R \left[\left(\frac{\varepsilon_d + \varepsilon_m}{\varepsilon_d \cdot \varepsilon_m} \right)^{1/2} \right] \quad (3)$$

Here, $\varepsilon_d = 1$ represents the dielectric constant of the medium, $\varepsilon_m = (n + ik)$ signifies the dielectric constant of the metal, λ denotes the wavelength of the incident laser, n stands for the refractive index of the metal, and k represents the extinction coefficient or an approximation thereof. Considering the refractive index and extinction coefficient of niobium at 1064 nm, with n=1.75 and k=5.45 [13], respectively, the calculated value of the plasmon wavelength ($\lambda_{SPP} = 800\ nm$) aligns closely with most periods observed in our experiments. However, this refractive index value was derived from the smooth surface of Nb crystals at room temperature. The obtained values of the refractive index at the room temerature may not be applicable when working with metals exposed to high intensity femtosecond laser pulses or coated with nano/microstructures or oxide compounds. As a result, in such situations it may be necessary to consider alternative methods for obtaining accurate refractive index values. Regarding Nb alloy surface roughness, it is important to recognize that this factor can influence the actual portion of the effective refractive index at the metal/air interface, hence reducing the pulsation period [19]. In addition, the absorption of bcc transition metals at frequencies below 0.5 eV can be described as interband transitions. Therefore, to accurately estimate the dielectric constant value, it is necessary to take into account both the Drude model and the interband response.

4 Conclusion

This study investigated the effect of laser energy density on the distribution of LIPSS on the surface of niobium alloys. The study demonstrates the variation of LIPSS periodicity by correlating electron density in laser-induced plasma with the wavelength of surface plasmon waves. In the case the plasma induced on the surface of Nb alloy containng light carbon atoms, the free-electron concentration was not sufficient to influence the frequency of LIPSS at the wide ranges of the laser fluences. Beside, it can be concluded that alloys with heavy metals are capable of generating plasma containing highly concentrated free electrons, which regulates the dispersion parameters on the target surface. These relationships between electron density, laser-induced plasma dispersion parameters, and LIPSS periodicity are analyzed. It was found that

References

1. J. Huang, J. Zhang, W. Wang, X. Wang, Y. Cao, Z. Guo, Front. Phys. **10**, 932284 (2022).
2. Y. Nykyruy, S. Mudry, I. Shtablavyi, I. Gnilitskyi, Appl. Nanosci. **12**, 1337 (2022).
3. D. Milovanović, B. Gaković, Z. Popović, M. Momčilović, I. Radović, J. Limpouch, S. Petrović, Eur. Phys. J. D **76(2)**, 1-9 (2022).
4. J. Bonse, S.V. Kirner, J. Krüger, *Laser-Induced Periodic Surface Structures (LIPSS)* in: Handbook of Laser Micro- and Nano-Engineering, K. Sugioka (Ed.), (Springer International Publishing, 2020).
5. A.S. Alnaser, S.A. Khan, R.A. Ganeev, E. Stratakis, Appl. Sci. **9**, 1554 (2019).
6. M. Huang, F. Zhao, Y. Cheng, N. Xu, Z. Xu, ACS Nano **3**, 4062 (2009).
7. A. Cubero, E. Martínez, L.L. Plantard, R. Sánchez-Martín, M. Manso-Silván, J.L. Sanz, J.M. Vázquez de Parga, R.J. Martín-Palma, Appl. Surf. Sci. **508,** 145140 (2020).
8. C. Florian, S.V. Kirner, J. Krüger, J. Bonse, J. Laser Appl. **32(4),** 042003 (2020).
9. E.E. Nikishina, D.V. Drobot, E.N. Lebedeva, Russ. J. Non-Ferrous Met. **54**, 446 (2013).

10. L. Sun, X. Liu, X. Xu, S. Lei, H. Li, Q. Zhai, J. Iron Steel Res. Int. **29**, 1513 (2022).
11. R. Grill, A. Gnadenberger, Int. J. Refract. Met. Hard Mater. **24**, 275 (2006).
12. C. Laverick, J. Less Common Met. **139**, 107 (1988).
13. A. Pan, A. Dias, M. Gomez-Aranzadi, S.M. Olaizola, A. Rodriguez, J. Appl. Phys. **115**, 173101 (2014).
14. A. Cubero, L. Martínez, E. Martínez, M. Manso-Silván, J.L. Sanz, J.M. Vázquez de Parga, R.J. Martín-Palma, Nanomaterials **10(12),** 2525 (2020).
15. S. Khaple, U. Prakash, B.R. Golla, V.V. Satya Prasad, Metallogr. Microstruct. Anal. **9**, 127 (2020).
16. P.R. West, S. Ishii, G.V. Naik, N.K. Emani, V.M. Shalaev, A. Boltasseva, Laser & Photonics Rev. **4**, 795 (2010).
17. N. Ackerl, K. Wegener, J. Laser Appl. **32(2)**, 022049 (2020).
18. G.S. Boltaev, M. Iqbal, S.R. Kamalov, M. Vapaev, I.Y. Davletov, A.S. Alnaser, Appl. Phys. A **128**, 488 (2022).
19. A.Y. Vorobyev, C. Guo, J. Appl. Phys. **104**, 063523 (2008).